

# Parametric amplification of few-cycle carrier-envelope phase-stable pulses at 2.1 $\mu\text{m}$

T. Fuji, N. Ishii, C. Y. Teisset, X. Gu, Th. Metzger, and A. Baltuška

Max-Planck-Institut für Quantenoptik, Hans-Kopfermann-Strasse 1, D-85748 Garching, Germany

N. Forget and D. Kaplan

Fastlite, Bâtiment 403, Ecole Polytechnique, 91128 Palaiseau, France

A. Galvanauskas

Department of Electrical Engineering and Computer Science, College of Engineering, University of Michigan, 1301 Beal Avenue, Ann Arbor, Michigan 48109-2122

F. Krausz\*

Ludwig-Maximilians-Universität München, Am Coulombwall 1, D-85748 Garching, Germany

Received December 9, 2005; accepted December 23, 2005; posted January 27, 2006 (Doc. ID 66564)

We demonstrate an optical parametric chirped-pulse amplifier producing infrared 20 fs (3-optical-cycle) pulses with a stable carrier-envelope phase. The amplifier is seeded with self-phase-stabilized pulses obtained by optical rectification of the output of an ultrabroadband Ti:sapphire oscillator. Energies of  $\sim 80 \mu\text{J}$  with a well-suppressed background of parametric superfluorescence and up to  $400 \mu\text{J}$  with a superfluorescence background are obtained from a two-stage parametric amplifier based on periodically poled  $\text{LiNbO}_3$  and  $\text{LiTaO}_3$  crystals. The parametric amplifier is pumped by an optically synchronized 1 kHz, 30 ps, 1053 nm Nd:YLF amplifier seeded by the same Ti:sapphire oscillator. © 2006 Optical Society of America  
OCIS codes: 190.4970, 320.5520, 140.3070.

Rapid advances in high-field physics have been achieved in recent years, particularly in the reproducible generation of isolated soft-x-ray attosecond pulses,<sup>1</sup> as a result of the development of drive lasers with specialized pulse properties. These properties include ultrahigh peak intensity, quasi-monocycle duration, and reliable control over the carrier-envelope phase (CEP).<sup>2</sup> While existing drive lasers operate near  $0.8 \mu\text{m}$ , in the gain region of the Ti:sapphire, operating at longer, infrared wavelengths would be advantageous because the ponderomotive energy scales with  $\lambda^2$ . Therefore, the intensity of driving laser pulses needed to attain higher-order harmonic generation at a given x-ray photon energy can be substantially lower in comparison with the  $0.8 \mu\text{m}$  case.<sup>3–5</sup> The use of IR drive pulses should extend the cutoff energy of x-ray photons and yield even shorter attosecond x-ray pulses. From the standpoint of laser technology, the longer duration of the IR optical period reduces the number of cycles for a given pulse envelope and, therefore, relaxes the requirement for amplifier gain bandwidth.

The concept of optical parametric chirped-pulse amplification<sup>6,7</sup> (OPCPA) could be ideal for future development of intense ultrashort-pulse higher-harmonic generation drive sources. Recently, several OPCPA systems delivering few-cycle  $0.8 \mu\text{m}$  pulses were reported.<sup>8–11</sup> Femtosecond IR OPCPA systems have also been demonstrated,<sup>12–14</sup> but not in the few-cycle pulse range. In this Letter we describe a prototype few-cycle CEP-stabilized IR OPCPA based on periodically poled crystals.

A schematic of our two-stage OPCPA is presented in Fig. 1. The pump laser consists of a home-built 30 ps, 1053 nm Nd:YLF regenerative amplifier and a 4-pass postamplifier, delivering pulses up to 10 mJ at 1 kHz repetition rate. The pump pulses are optically synchronized with the seed pulses of OPCPA by injection seeding from a broadband Ti:sapphire oscillator.<sup>15</sup> The output spectrum of the 5 nJ, 6 fs all-chirped-mirror Ti:sapphire oscillator is given elsewhere.<sup>16</sup> The oscillator pulse energy within the fluorescence bandwidth of Nd:YLF at 1053 nm, diverted for optical seeding of the regenerative amplifier, is  $\sim 2 \text{ pJ}$ .

IR seed pulses for the OPCPA are produced by difference-frequency generation (DFG) of the output of the Ti:sapphire oscillator in a 1 mm long MgO-doped periodically poled  $\text{LiNbO}_3$  crystal (PPLN) with a quasi-phase-matching period of  $\Lambda_{\text{QPM}} = 13.9 \mu\text{m}$ . The resultant DFG spectrum is shown as a dashed curve in Fig. 2. The estimated energy in the IR seed pulse is 4 pJ without heating the DFG crystal. The three-wave mixing process in DFG is identical to op-

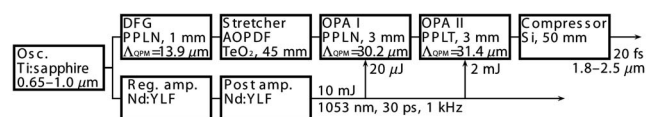


Fig. 1. Schematic of the IR OPCPA. AOPDF, acousto-optic programmable dispersive filter (Dazzler; Fastlite, Ltd.); PPLN, periodically poled  $\text{LiNbO}_3$  crystal; PPLT, periodically poled  $\text{LiTaO}_3$  crystal. All periodically poled crystals were obtained from HC Photonics, Ltd.

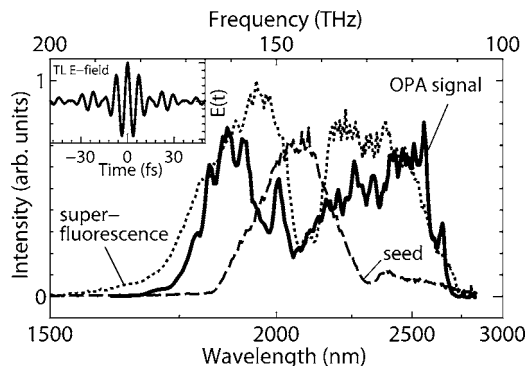


Fig. 2. Summary of spectral properties of the IR OPCPA. Solid curve, amplified signal spectrum after the second OPA stage; dashed curve, spectrum of the seed pulse generated by difference-frequency mixing; dotted curve, superfluorescence spectrum in a 3 mm thick PPLN. Inset, electric field of the pulse calculated for the solid curve assuming ideal pulse compression.

tical rectification, therefore, the pulses generated via DFG carry a constant CEP offset.<sup>17–19</sup> Unlike DFG schemes that mix two frequency-shifted pulses,<sup>19</sup> DFG between short- and long-wavelength components of a single broadband pulse removes the necessity to maintain a constant time delay between the mixing pulses. Consequently, there is no delay-related source of CEP jitter in our system.

Our optical parametric amplifier (OPA) operates near the degeneracy point of the three-wave mixing to ensure the broadest possible gain<sup>20</sup> in periodically poled nonlinear crystals. The first stage of the two-stage amplifier employs a 3 mm thick periodically poled MgO-doped LiNbO<sub>3</sub> crystal (PPLN OPA I in Fig. 1,  $\Lambda_{\text{QPM}}=30.2 \mu\text{m}$ ). The crystal is heated to 200 °C to minimize the parasitic photorefractive effect. In the second-stage amplifier we use a periodically poled MgO-doped LiTaO<sub>3</sub> crystal (PPLT OPA II in Fig. 1,  $\Lambda_{\text{QPM}}=31.4 \mu\text{m}$ ). Compared with PPLN, the PPLT crystal has a lower nonlinear coefficient and, for the same crystal thickness, a slightly narrower phase-matching bandwidth. However, PPLT exhibits a higher damage threshold and has considerably smaller photorefractivity. The ultimate gain bandwidth potentially obtainable in our system is illustrated by the spectrum of parametric superfluorescence (dotted curve in Fig. 2) measured behind OPA I. For this measurement, the external OPA seed was blocked and a higher pump intensity was applied to switch to the regime of the optical parametric generator. The Fourier-limited pulse duration of this spectrum is  $\sim 12$  fs.

In both OPA stages we introduced a 1.5° noncollinearity angle (internal) between the pump and the seed beams. A small crossing angle is required for spatial separation of the otherwise degenerate signal and idler waves and to prevent their mutual interference. The  $1/e^2$  pump beam diameters are  $\sim 150$  and  $\sim 350 \mu\text{m}$  for the first and the second OPA stages, respectively. In OPA I, the signal pulse is amplified to 1.35  $\mu\text{J}$  with a 40  $\mu\text{J}$  pump. In OPA II, the signal energy is boosted to 0.4 mJ using a 5 mJ pump pulse. The pump energy in this case is limited by optical

damage to the PPLT crystal. The stability of the amplified pulse energy is 5% rms. Prior to amplification, the seed pulse was stretched to  $\sim 10$  ps in a 50 mm long antireflection-coated silicon block to maximize the efficiency of the pump energy conversion. The corresponding amplified spectrum is shown in Fig. 2 (solid curve). Gain saturation causes substantial broadening of the injected seed spectrum. A single-pass parametric gain in excess of  $10^6$  can be easily obtained in our system. However, this amplification regime corresponds to a nonnegligible amount of superfluorescence that competes with the injected seed pulse. Therefore, for further amplification, the signal has to be injected into subsequent parametric amplifier stages with correspondingly increased pump pulse energies.

Several options for the pulse stretcher–compressor pair can be considered. Both the pulse stretcher and the compressor of an IR chirped-pulse amplifier could be based on bulk-dispersion materials,<sup>21</sup> because several types of glass (fused silica, fluoride glass, etc.) exhibit negative dispersion in this spectral range. However, it is impossible for compression from  $\sim 10$  ps to  $<20$  fs, which is a few cycles for IR pulses, since the sign of the third-order dispersion is the same for the materials with both positive and negative linear dispersion. To achieve few-cycle operation in this work, we employ an IR acousto-optic programmable dispersive filter Dazzler (Fastlite, Ltd.) as a pulse stretcher in front of the OPA and recompress the pulse in the above-mentioned 50 mm thick Si block. Because of the low material dispersion in the IR in comparison with the typically used near-IR spectral range, our 1.3–2.5  $\mu\text{m}$  Dazzler can fully compensate for both the internal dispersion of a 45-mm TeO<sub>2</sub> crystal and its dispersion of the Si block. The diffraction efficiency of the broadband Dazzler is  $\sim 10\%$ , which dramatically reduces the seed energy supplied to the OPA. Therefore, the pump energies of both OPA stages have to be reduced correspondingly to suppress amplification of superfluorescence. As a result, the usable signal energy at the output of OPA II is decreased to  $\sim 80 \mu\text{J}$ .

The amplified pulse is compressed in the Si block without significant loss. The pulse width is measured with an autocorrelator based on two-photon-induced photocurrent<sup>22</sup> in an InGaAs photodetector. The measured interferometric autocorrelation trace is shown in Fig. 3. The pulse appears to be compressed nearly to its theoretical limit, i.e.,  $\sim 20$  fs, or 3 cycles at FWHM. Since the wavelength range supported by the Dazzler is blueshifted with respect to the OPA gain bandwidth, the resultant amplified spectrum (Fig. 3, inset) is clipped around 2.5  $\mu\text{m}$ . Therefore, further reduction of the pulse duration is expected with a modified Dazzler that will cover the entire bandwidth of interest.

To characterize the CEP stability of the OPCPA system, we measured  $f$ -to- $3f$  spectral interferograms in a specially designed nonlinear interferometer. A 1 mm thick type I phase-matching  $\beta$ -barium borate crystal for third-harmonic generation<sup>23</sup> was placed in one arm of the interferometer, and a 2-mm-thick sap-

phire window for white-light generation in the other. The resultant spectral fringes, observed around 680 nm, are depicted in Fig. 4. The CEP dependence was verified by varying the glass thickness in front of the nonlinear interferometer. The residual phase excursions, seen in Fig. 4(b), are attributed to the amplitude–phase noise coupling in the white-light generator of the nonlinear interferometer.

In summary, we have demonstrated what is to our knowledge the first CEP-stable chirped-pulse parametric amplifier that currently produces 3-cycle pulses at the central wavelength of 2.1  $\mu\text{m}$ . The laser output is directly scalable with pump pulse energy and crystal size.<sup>24</sup> This scheme presents a promising route toward constructing a high-peak-power IR drive laser for high-field and attosecond applications.

This work was supported by the LaserLab Europe and XTRA European networks. We thank HC Photonics for fruitful discussions on periodically poled crystals. This research was greatly motivated by a proposal of L. DiMauro from Ohio State University for improved attosecond high-harmonic generation with an IR driver. T. Fuji's e-mail address is tkf@mpq.mpg.de.

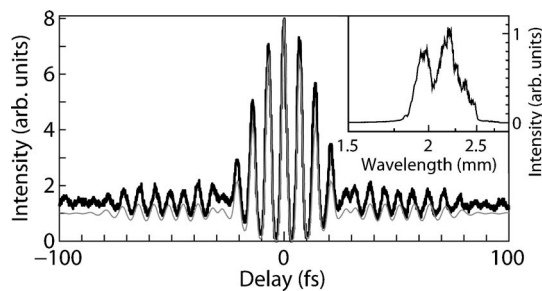


Fig. 3. Adaptive pulse compression using a Dazzler. Thick curve, measured interferometric autocorrelation based on the two-photon-induced photocurrent in an InGaAs photodiode; thin curve, calculated autocorrelation trace assuming ideal pulse compression. Inset, signal pulse spectrum.

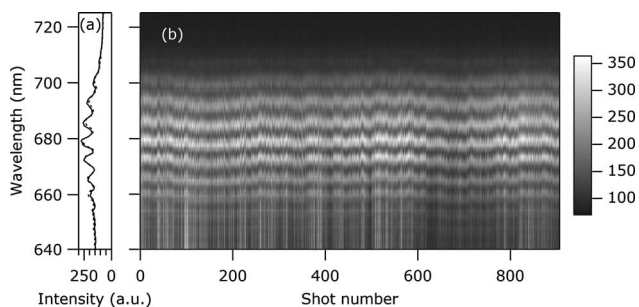


Fig. 4. Examination of CEP stability by nonlinear spectral interferometry. (a) Single-shot  $f$ -to- $3f$  interferogram (solid curve) and an average over 1 s (dashed curve). (b) Single-shot interferograms for successive laser shots. See text for details.

\*Also with the Max Planck Institute of Quantum Optics, Hans-Kopfermann-Strasse 1, D-85748 Garching, Germany, and the Photonics Institute, Vienna University of Technology, Gusshausstrasse 27/387, A-1040 Vienna, Austria.

## References

1. R. Kienberger, E. Goulielmakis, M. Uiberacker, A. Baltuška, V. S. Yakovlev, F. Bammer, A. Scrinzi, T. Westerwalbesloh, U. Kleineberg, U. Heinzmann, M. Drescher, and F. Krausz, *Nature* **427**, 817 (2004).
2. A. Baltuška, T. Udem, M. Uiberacker, M. Hentschel, E. Goulielmakis, C. Gohle, R. Holzwarth, V. S. Yakovlev, A. Scrinzi, T. W. Hänsch, and F. Krausz, *Nature* **421**, 611 (2003).
3. P. Agostini and L. F. DiMauro, *Rep. Prog. Phys.* **67**, 1 (2004).
4. M. Lewenstein, P. Balcou, M. Y. Ivanov, A. L'Huillier, and P. B. Corkum, *Phys. Rev. A* **49**, 2117 (1994).
5. A. Gordon and F. X. Kärtner, *Opt. Express* **13**, 2941 (2005).
6. A. Dubietis, G. Jonušauskas, and A. Piskarskas, *Opt. Commun.* **88**, 437 (1992).
7. I. N. Ross, P. Matousek, M. Towrie, A. J. Langley, and J. L. Collier, *Opt. Commun.* **144**, 125 (1997).
8. C. P. Hauri, P. Schlup, G. Arisholm, J. Biegert, and U. Keller, *Opt. Lett.* **29**, 1369 (2004).
9. R. T. Zinkstok, S. Witte, W. Hogervorst, and K. S. E. Eikema, *Opt. Lett.* **30**, 78 (2005).
10. N. Ishii, L. Turi, V. S. Yakovlev, T. Fuji, F. Krausz, A. Baltuška, R. Butkus, G. Veitas, V. Smilgevičius, R. Danielius, and A. Piskarskas, *Opt. Lett.* **30**, 567 (2005).
11. S. Witte, R. T. Zinkstok, W. Hogervorst, and K. S. E. Eikema, *Opt. Express* **13**, 4903 (2005).
12. A. Galvanauskas, A. Hariharan, D. Harter, M. A. Arbore, and M. M. Fejer, *Opt. Lett.* **23**, 210 (1998).
13. F. Rotermund, C. J. Yoon, V. Petrov, F. Noack, S. Kurimura, N.-E. Yu, and K. Kitamura, *Opt. Express* **12**, 6421 (2004).
14. J. V. Rudd, R. J. Law, T. S. Luk, and S. M. Cameron, *Opt. Lett.* **30**, 1974 (2005).
15. N. Ishii, C. Y. Teisset, T. Fuji, S. Köhler, K. Schmid, L. Veisz, A. Baltuška, and F. Krausz, "Seeding of the 11-fs OPCPA and its  $\text{Nd}^{3+}$  picosecond pump laser from a single broadband Ti:sapphire oscillator," *IEEE Sel. Top. Quantum Electron* (to be published).
16. T. Fuji, J. Rauschenberger, C. Gohle, A. Apolonski, T. Udem, V. S. Yakovlev, G. Tempea, T. W. Hänsch, and F. Krausz, *New J. Phys.* **7**, 116 (2005).
17. A. Baltuška, T. Fuji, and T. Kobayashi, *Phys. Rev. Lett.* **88**, 133901 (2002).
18. T. Fuji, A. Apolonski, and F. Krausz, *Opt. Lett.* **29**, 632 (2004).
19. C. Manzoni, G. Cerullo, and S. D. Silvestri, *Opt. Lett.* **29**, 2668 (2004).
20. J. Limpert, C. Aguergaray, S. Montant, I. Manek-Hönninger, S. Petit, D. Descamps, E. Cormier, and F. Salin, *Opt. Express* **13**, 7386 (2005).
21. N. Demirdöven, M. Khalil, O. Golonzka, and A. Tokmakoff, *Opt. Lett.* **27**, 433 (2002).
22. J. K. Ranka, A. L. Gaeta, A. Baltuška, M. S. Pshenichnikov, and D. A. Wiersma, *Opt. Lett.* **22**, 1344 (1997).
23. P. S. Banks, M. D. Feit, and M. D. Perry, *Opt. Lett.* **24**, 4 (1999).
24. H. Ishizuki and T. Taira, *Opt. Lett.* **30**, 2918 (2005).